

High-intensity Focused Ultrasound In Interventricular Septal Myocardial Ablation: Effects Of Coronary Flow

Fei Ren

Shandong University School of Medicine: Shandong University Cheeloo College of Medicine

Yulong Sui

Qingdao University Medical College

Xiaobo Gong

Chongqing University of Medical Science: Chongqing Medical University

Quansheng Xing (✉ xingqs0532@163.com)

Qingdao Women and Children's Hospital <https://orcid.org/0000-0002-0171-801X>

Zhibiao Wang

Chongqing University of Medical Science: Chongqing Medical University

Research Article

Keywords: High-intensity focused ultrasound, Septal ablation, coronary blood

Posted Date: June 9th, 2022

DOI: <https://doi.org/10.21203/rs.3.rs-1235136/v1>

License:  This work is licensed under a Creative Commons Attribution 4.0 International License. [Read Full License](#)

Abstract

Background

High-intensity focused ultrasound (HIFU) can generate necrotic damage in deep tissues through thermal ablation and cavitation, without significant damage to the surrounding tissues. The high blood perfusion of heat affects the deposition of energy. The aim of this study was to evaluate the effect of cooling of coronary blood flow for high-intensity focused ultrasound ablation.

Methods

Continuous and pulsed HIFU (2000 J) at duty cycles (DCs) of 100% and 20% were examined for their capacity to ablate the perfused porcine heart tissue in vitro. After ablation, gray scale changes and pathological features were observed or measured, and tissue necrosis area and volume were calculated.

Results

The cardiomyocytes in the lesions underwent necrosis with a clear boundary. The endocardium was intact without necrosis. The three-dimensional morphology of the lesions appeared approximately as ellipsoids. With the increase of perfusion speed, the necrotic volume in the target area was gradually reduced.

Conclusions

HIFU has the potential to become a new minimally invasive surgery for ventricular septal myocardial ablation. Reducing coronary blood flow can improve the ablation effect.

1. Introduction

High-intensity focused ultrasound (HIFU) is a new non-invasive treatment technology that generates necrotic damage in deep tissues through thermal ablation and cavitation, without significant damage to the surrounding tissues [1]. Due to its safe and non-invasive nature, it is widely used in clinical practice, especially to treat uterine, prostate, breast, and liver tumours, as well as osteogenic sarcoma [2–4]. Compared with traditional surgery, HIFU has many significant advantages, such as no wounds, less postoperative pain and discomfort, a lower requirement for blood transfusion, and a lower incidence of postoperative complications, which may be due to its non-invasive features.

In the last 20 years, investigations into the application of HIFU in the cardiovascular field have been ongoing, mainly including myocardial ablation and electrophysiological ablation [5–7]. Previous studies have established several pathways, including thoracotomy [8], transthoracic [9], trans-vascular [10], and transesophageal [11]. In 2007, Boris Schmidt first reported the use of a steerable HIFU balloon catheter for radiofrequency ablation (RFA) of the pulmonary vein ostium in patients with atrial fibrillation, with the success rate of pulmonary vein isolation reaching 89% [12]. Subsequently, the products related to pulmonary vein isolation by HIFU appeared one after another. However, with the improvement in the postoperative follow-up, we found that the incidence of phrenic nerve and left atrial-esophageal fistula was higher, so all the related products have been introduced into clinical treatment [13–14]. Due to the special location of the heart, mobility, and rich blood flow, HIFU has not been applied in the field of cardiovascular disease.

Because the heart is an organ with high blood perfusion, whose blood vessels act as heat sinks, it is necessary to evaluate the effect of cooling of the coronary blood flow for HIFU ablation. In this study, freshly isolated porcine hearts were perfused through the coronary artery. Under the condition of regulating different perfusion flows, the coagulative necrosis volume changes of myocardial tissue after HIFU ablation were observed to study the effect of coronary blood flow for HIFU myocardial ablation. Our study provides an experimental basis for the application of HIFU in the cardiovascular field.

2. Methods

2.1 HIFU Apparatus

The JC200 HIFU tumour treatment system used in this experimental study has been used many times in cardiovascular research (Figure 1). It mainly comprises the following components: an operation control system (a), a treatment bed (b), a treatment probe with a diameter of 220 mm (c), an ultrasonic image probe (c), and a degassed water generation unit (d). The treatment probe of the device had an effective focal length of 148 mm and an operating frequency of 1.03 MHz. The focal region in physics is an ellipsoid with a long axis of 10 mm and a short axis of 2 mm. The sound power of the treatment probe was continuously adjustable from 24–450 W, and the sound intensity at the focus was from 1.2–22.5 KW/cm². The time for a single energy release was accurate in milliseconds. The imaging probe was in the middle of the therapeutic probe, with a frequency of 3.5 MHz. The imaging system is integrated with the MyLab30 colour Doppler ultrasound diagnosis system and HIFU treatment system, which can guide the localisation and ablation of high-intensity focused ultrasound. The integrated HIFU probe was immersed in the degassed water tank, and degassed water was used as the coupling medium for HIFU therapy.

2.2 Heart Preparation

The experimental protocol was approved by the institutional ethics committee of Chongqing Medical University. The porcine hearts were removed within 5 min after sacrifice, and 20 hearts weighing 400–500 g were selected. Immediately, 500 ml of high potassium myocardial protection solution containing 25 u/ml of heparin was slowly injected through the coronary artery to expel blood from the myocardium and prevent thrombosis. The processed porcine hearts were stored at 4°C and sent to the laboratory.

2.3 Ablation Protocol

- a. The porcine hearts were degassed for 30 min in a degassing cylinder and then placed in a 37°C degassing water tank. The coronary perfusion tube was inserted into the bilateral coronary arteries, and 37°C degassed normal saline was injected through the peristaltic pump during ablation.
- b. The imaging monitoring system was set to real-time status (real-time observation throughout the ablation procedure). The treatment target was positioned in the upper segment of the ventricular septum under the aortic valve.
- c. Different irradiation powers and irradiation times were applied to these porcine hearts to generate two different treatment groups (Figure 2). Group A: power of 200 for 10 s; Group B: power of 400 W for 20 s with a pulse work of 200 ms in 800 ms. The upper interventricular septum of each porcine heart was ablated once in a peristaltic pump at 0 ml/min, 50 ml/min, 150 ml/min, and 250 ml/min, respectively.

2.4 Ablation Lesion Measurement

The ablated porcine ventricular septum was cut with a thickness of 1–2 mm along the acoustic axis to find the largest injury surface in the target area, and a ruler was placed under the specimen to capture its image with a digital camera under direct vision. The ablation lesion volume was calculated using the HIFU software (Chongqing Haifu, China).

2.5 Histological Examination

Porcine heart tissues were fixed in 4% formalin for a minimum of 24 h and were embedded in paraffin blocks after dehydration. The paraffin blocks were sectioned into slices, and standard hematoxylin-eosin staining was performed for histological observation under an optical microscope. Morphological changes and staining of the cells in the necrotic area were observed.

2.6 Statistical Analysis

Under different perfusion flow conditions, the length, width and area of the maximum coagulative necrosis surface and the volume of coagulative necrosis were recorded. SPSS software (version 19.0; IBM Corporation, Armonk, NY) was used for statistical analysis. Data are expressed as the mean±standard deviation. A one-way analysis of variance was used for comparisons among the groups, and the least significant difference test was used for post hoc pair-wise comparisons. Statistical significance was set at $P < 0.05$.

3. Results

3.1 Gross Observation of Cardiac Tissue Necrosis After Ablation

After a series of ablations, there were four coagulative necrotic lesions of different sizes with a clear boundary in the ventricular septum of each porcine heart. The shape of the necrotic lesion was similar to an ellipse, and its colour was significantly different from that of the surrounding normal myocardial tissue, which was dark red, and the target tissue became gray-white after irradiation (Figure 3A). The endocardial surface was intact, and no significant damage was observed on the endocardial surface (Figure 3B). The extent of coagulative necrosis at the target area was measured using Jupiter software, as shown in Table 1. The size of the necrotic areas differed under different perfusion flows. With the increase in perfusion speed, the necrotic volume in the target area gradually decreased (Figure 4). Figure 3. Gross morphologic features of the lesions. A: four coagulative necrotic lesions of different sizes with a clear boundary in the ventricular septum. The color of the necrotic lesion was significantly different from that of the surrounding normal myocardial tissue. B: The endocardial surface was intact, and no significant damage was seen in the endocardial surface.

Table 1. Ablation results from the experiment

parameter	Group A a power of 200W for 10 seconds				Group B a power of 400W for 20 seconds with a pulse work of 200ms in 800ms			
	Necrosis Length(mm)	Necrosis width (mm)	Necrosis area (mm ²)	Necrosis volume (mm ³)	Necrosis length (mm)	Necrosis width (mm)	Necrosis area (mm ²)	Necrosis volume (mm ³)
0 ml/min	9.68±1.43	4.21±0.43	27.52±6.26	129.14±45.68	9.62±1.65	3.56±0.93	23.94±7.90	110±52.72
50 ml/min	8.48±1.23	3.83±0.74	21.12±6.13	88.93±37.22	8.24±1.08	3.28±0.81	17.66±4.81	67.91±26.91
150ml/min	6.45±1.09	3.12±0.53	13.19±5.03	43.86±22.75	6.85±1.4	2.84±0.67	12.78±4.51	43.67±20.93
250ml/min	5.0±1.31	2.23±0.71	7.71±3.7	20.51±12.71	5.4±0.91	2.45±0.63	8.48±3.14	23±11.96
P	<0.001	<0.001	<0.001	<0.001	<0.001	0.021	<0.001	<0.001
HIFU Dose consumption (J)	2000	2000	2000	2000	2000	2000	2000	2000

3.2 Grayscale Changes Under B-Mode US Monitoring

Real-time ultrasound images showed that the grey scale of the target tissue was constantly changing during radiation (Figure 5). At the beginning of irradiation, the grey level of the target area did not change significantly, but with increasing irradiation time, it began to increase. The grey level then decreased, but increased again after continuous irradiation. The grey of the target tissue exhibited a dynamic change process until the irradiation stopped (i.e. no change—enhancement—reduction—re-enhancement), and the grey level was always changed within the target range during the entire irradiation process.

Histologic Features:

Under a low-power light microscope, the coagulative necrosis area was clearly demarcated from the surrounding normal tissues (Figure 6a). The necrotic area was separated from the surrounding normal myocardium by one to three morphologically abnormal cell populations. The myocardial cells in normal tissues are arranged regularly. In the necrotic area, myofibers showed degeneration and necrosis, with vague cell structure and disordered arrangement. In addition, fractured myocardial fibers and flaky irregular granular structure could be seen in some necrotic areas.

In the high-power light microscope, the morphology of myocardial cells in the ablation lesion was significantly changed, and the normal structure of cells was also lost (Figure 6b & Figure 6c). The cardiomyocytes underwent obvious cell death changes such as karyopycnosis, fragmentation, dissolution or disappearance of nuclei and only a few morphologically normal interstitial nuclei remained. Myocardial fibers were arranged disorderly, with vague outline and dissolution or disappearance of transverse striations. Peripheral normal myocardial cells were arranged neatly, with complete structure and normal nucleus (Figure 6d). Endocardium connectivity was intact and endothelial cell morphology was normal.

4. Discussion

Cardiovascular disease is currently the most common cause of death worldwide, affecting approximately twice as many people as cancer, with increasing social and economic burden as the population ages [15]. Hypertrophic cardiomyopathy (HCM) is a myocardial

disease of unknown cause, characterised by asymmetric hypertrophy of the ventricular wall, invasion of the interventricular septum, diminution of the intraventricular cavity, obstruction of left ventricular blood filling, and decreased left ventricular diastolic compliance. According to the presence or absence of obstruction of the left ventricular outflow tract, it is divided into obstructive and non-obstructive hypertrophic cardiomyopathy, which may be related to heredity. It is a common hereditary cardiomyopathy, with an incidence rate of approximately 0.2% of the total population^[16]. About 70% of HCMs present with left ventricular outflow tract obstruction in resting or stimulated states, leading to dyspnea, chest pain, atrial fibrillation, heart failure, and even sudden death. Interventricular septal myocardial reduction (SRT) is effective for treating HCM, including surgical treatment^[17], alcohol isolation^[18], and RFA^[19]. All current myocardial volume reduction strategies are invasive, with high surgical risk and the possibility of serious surgical complications; therefore, most patients with HCM choose medication instead of surgery.

HIFU transmits low ultrasonic energy from outside the body, which transmits through the skin and the corresponding tissues to reach a target area in the body, so that the energy focused in the target area is extremely high. HIFU can cause target tissue cells to undergo coagulative necrosis in a short time through thermal, cavitation, and mechanical effects, and other mechanisms, and has little or no damage to the tissues on the acoustic channel and around the target area, thereby achieving non-invasive ablation. Third, mechanical effect refers to the mechanical effect that ultrasonic energy can generate with high-speed vibrations back and forth, which can cause cell autolysis, DNA molecular degradation, and apoptosis^[20]. Thermal effects play a major role in the mechanism of HIFU ablation. Ultrasonic energy is absorbed by the tissue and converted into heat, which causes the temperature of the target tissue to rise to the threshold temperature of irreversible damage in a short time, leading to irreversible tissue cell death. Cavitation also plays an important role in this process. Cavitation is a dynamic process in which tiny bubbles in the target tissue repeatedly oscillate, expand, contract, and finally break under the action of ultrasound. A large amount of energy is released during this process because of the cavitation effect of the tissue. When the cavitation microbubbles collapse, extreme physical effects (such as high temperature, high pressure, strong shock waves, etc.) can be locally generated to destroy cell membrane structures and organelles, resulting in cell death^[21]. Finally, ultrasonic waves generate mechanical action with high-speed oscillation, which can cause cell autolysis, DNA molecular degradation, and apoptosis, thereby killing cells. Based on these mechanisms of action of HIFU, HIFU shows the advantages of non-invasive and accurate positioning in clinical treatment, and has been widely used in the treatment of clinical tumours^[22]. Intracardiac lesions using HIFU were demonstrated for the first time in an in vitro study, in which 2-6 mm focal lesions in the medial wall of the myocardium were produced without damage to surrounding tissues^[23]. In the last 20 years, the application of HIFU in the cardiovascular field has been ongoing. In 2007, Otsuka used HIFU with ECG-gated technology to ablate the interventricular septum myocardium in dogs after thoracotomy, and confirmed that HIFU could produce targeted and well-demarcated thermal damage in the moving heart^[24]. Boris Schmidt first reported the clinical application of the HIFU catheter for pulmonary vein isolation to treat atrial fibrillation in 2007^[25]. However, later clinical studies showed that complications such as phrenic nerve injury and left atrial esophageal fistula may occur after surgery. In 2013, Elodie Constanciel designed a HIFU probe guided by transesophageal ultrasound, which verified the safety and feasibility of the transesophageal approach^[26]. In 2013, Huang Jing used pleural effusion to establish an artificial channel, and HIFU was used to ablate the ventricular septal myocardium in dogs through the thoracic cavity^[5]. Although previous studies have been performed via multiple pathways, including thoracotomy, transthoracic, and transesophageal, they have not been clinically applied due to various limitations.

Due to the anatomical location and particularity of the heart, it was once considered a restricted area for HIFU ablation. The main reasons for this are as follows. First, the heart is surrounded by gas-rich lungs in the thoracic cavity, which consists of the sternum, ribs, and thoracic vertebrae. It is difficult for ultrasonic energy to penetrate these tissues to reach the heart and may cause damage to the surrounding tissues. Second, the heart is an organ with rapid and rhythmic movement, and its movement affects the accurate positioning of HIFU and energy deposition. Third, the heart is rich in blood flow, and owing to the cooling effect of blood flow, it is difficult for the heat generated by HIFU to precipitate in the myocardium. Therefore, these factors have hindered the application of HIFU in cardiovascular diseases. Previous studies have chosen transesophageal and intravascular pathways to avoid the influence of cardiac anatomical location and have made substantial progress.

Because the heart moves continuously and rhythmically, and there is no effective method for the focal area of HIFU to continuously track the moving target area, the pulse method can be used for HIFU ablation of myocardial tissue in motion. The pulse mode is discontinuous transmission, which adjusts the working and intermittent time according to the change in the cardiac cycle. The ventricular systolic period is about 0.2-0.3 s, when the ventricular wall and ventricular septum are thickened, which is convenient for target location. Moreover, the blood supply to the heart is in the diastolic period, and there is almost no blood flow in the systolic period. At this time, the heat generated by HIFU is not removed by the blood flow, and it is easily absorbed by the myocardium. Otsuka et al.

reported that HIFU using electrocardiogram gating can provide more accurate ablation in a beating heart [24]. Rong et al. reported that electrocardiogram-triggering ablation can further eliminate the influence of cardiac motion and believed that this technique could be applied to the treatment of cardiovascular diseases by HIFU [25].

The heart is a dynamic three-dimensional structure with abundant blood flow in the heart cavity and myocardium. The adult heart accounts for 0.5% of the body weight, while coronary blood flow accounts for 5% of the cardiac output. Therefore, the abundant blood flow in the myocardium seriously affects the ablation effect of HIFU. Previous studies have found that under the conditions of the same HIFU intensity and irradiation time, the heat generated in the blood-rich tissues would be quickly removed by the blood flow, and the extent of tissue necrosis would be affected [27]. An abundant vascular bed can not only reduce the peak temperature rise caused by HIFU, but also reduce the size and change the shape of the injury. This study shows that with a decrease in blood perfusion in the treatment area, the effect of hyperthermia is significantly improved, which is the same as in previous studies. Therefore, medical strategies to reduce or prevent blood flow into the treatment area have been proposed as areas of improvement for clinical treatment regimens. For example, when HIFU is used to treat uterine fibroids, the heat dissipation effect of fibroid blood vessels is reduced through the injection of oxycontin, which causes uterine contraction [28]. Myocardial ablation is an effective treatment for arrhythmia and hypertrophic cardiomyopathy, and transcatheter RFA has achieved great clinical success. HIFU may be a method for the treatment of hypertrophic obstructive cardiomyopathy in the future.

The myocardium of the left ventricular outflow tract was mainly supplied by the septal branches of the left coronary artery. When ablating the hypertrophic myocardium in the left ventricular outflow tract, septal branch occlusion can be used to reduce the blood supply to the hypertrophic myocardium and make the heat generated by HIFU more easily precipitate in the myocardium in this area, thereby increasing the effect of HIFU ablation.

5. Study Limitations

Firstly, this study is an in vitro experiment. Although it simulated coronary blood flow, it lacked the effects of heart movement and myocardial contraction. The other one, due to the in vitro experiment, the influence of the environment around the heart on the treatment effect was ignored. In the future, we will conduct experiments in animals via catheter or transesophageal pathway, to lay the foundation for further clinical trials.

6. Conclusion

Although there is rich experience in the therapeutic application of HIFU in patients with various tumours, its application in the cardiovascular field is rare but promising. In our study, we found that with a decrease in intramyocardial perfusion blood flow, the thermal therapeutic effect of HIFU was significantly improved. Septal branch occlusion can be used as a pretreatment to improve the efficacy of HIFU treatment for hypertrophic myocardial tissue. Although HIFU has not been studied in humans with HCM, it offers the possibility of a completely non-invasive treatment in the future.

Declarations

Acknowledgements

Not applicable.

Funding

This work is supported by The National Natural Science Foundation of China (NSFC) [Grant numbers 81770315, 82071583]; Taishan Scholars Program

Availability of data and materials

Not applicable.

Ethics approval and consent to participate

The work protocol was approved by the institutional ethics committee of Chongqing Medical University.

Consent for publication

Not applicable.

Competing interests

Not applicable.

References

1. Cheung TT, Ma KW, She WH. A review on radiofrequency, microwave and high-intensity focused ultrasound ablations for hepatocellular carcinoma with cirrhosis. *Hepatobiliary Surg Nutr.* 2021;10:193–209. DOI:10.21037/hbsn.2020.03.11.
2. Mohammadpour M, Firoozabadi B. Numerical study of the effect of vascular bed on heat transfer during high intensity focused ultrasound (HIFU) ablation of the liver tumor. *J Therm Biol.* 2019;86:102431. DOI:10.1016/j.jtherbio.2019.102431.
3. Sequeiros RB, Joronen K, Komar G, Seppo K, Koskinen. High intensity focused ultrasound (HIFU) in tumor therapy. *Duodecim.* 2017;13:143–9. DOI:10.1038/nrc1591.
4. Groen MHA, Slieker FJB, Vink A. Safety and feasibility of arterial wall targeting with robot-assisted high intensity focused ultrasound: a preclinical study. *Int J Hyperth.* 2020;37:903–12. DOI:10.1080/02656736.2020.1795278.
5. Rong S, Woo K, Zhou Q, Zhu Q, Wu Q, Wang Q, et al. Septal ablation induced by transthoracic high-intensity focused ultrasound in canines. *J Am Soc Echocardiogr.* 2013;26:1228–34. DOI:10.1016/j.echo.2013.06.020.
6. Miller DL, Lu X, Dou C, Zhu YI, Fuller R, Fabiilli ML. Ultrasonic cavitation-enabled treatment for therapy of hypertrophic cardiomyopathy: proof of principle. *Ultrasound Med Bio.* 2018;19:1439–50. DOI:10.1016/j.ultrasmedbio.2018.03.010.
7. Nazer B, Salgaonkar V, Diederich CJ, Jones PD, Duggirala S, Tanaka Y. Epicardial Catheter Ablation Using High-Intensity Ultrasound: Validation in a Swine Model. *Circ Arrhythm Electrophysiol.* 2015;8:1491–7. DOI:10.1161/CIRCEP.115.003547.
8. Zheng M, Shentu W, Dingzhang Chen. High-intensity focused ultrasound ablation of myocardium in vivo and instantaneous biological response. *Echocardiography.* 2014;31:1146–53. DOI: 10.1111/echo.12526.
9. Fei Lü W, Huang, David G, Benditt. A feasibility study of noninvasive ablation of ventricular tachycardia using high-intensity focused ultrasound. *J Cardiovasc Electrophysiol.* 2018;29:788–94. DOI:10.1111/jce.13459.
10. Kars Neven A, Metzner B, Schmidt F, Ouyang. Karl-Heinz Kuck. Two-year clinical follow-up after pulmonary vein isolation using high-intensity focused ultrasound (HIFU) and an esophageal temperature-guided safety algorithm. *Heart Rhythm.* 2012;9(3):407–13. DOI:10.1016/j.hrthm.2011.09.072.
11. Greillier P, Ankou B, Bour P, Zorgani A, Abell E, Romain Lacoste. Myocardial Thermal Ablation with a Transesophageal High-Intensity Focused Ultrasound Probe: Experiments on Beating Heart Models. *Ultrasound Med Biol.* 2018 Dec;44(12):2625–36. DOI:10.1016/j.ultrasmedbio.2018.06.013.
12. Boris Schmidt M, Antz S, Ernst F, Ouyang P, Falk, Julian KR, Chun. Pulmonary vein isolation by high-intensity focused ultrasound: First-in-man study with a steerable balloon catheter. *Heart Rhythm.* 2007;4(5):575–84. DOI:10.1016/j.hrthm.2007.01.017.
13. Jacob I, Laughner <background-color:#BCBCBC;usup>1</background-color:#BCBCBC;usup>, MS, Sulkin Z, Wu CX, Deng, Igor R Efimov Three Potential Mechanisms for Failure of High Intensity Focused Ultrasound Ablation in Cardiac Tissue. *Circ Arrhythm Electrophysiol.* 2012;5(2):409–16. DOI:10.1161/CIRCEP.111.967216. Epub. 2012 Feb 9.
14. Neven K, Metzner A, Schmidt B, Kuck KH. Two-year clinical follow-up after pulmonary vein isolation using high-intensity focused ultrasound (HIFU) and an esophageal temperature-guided safety algorithm. *Heart Rhythm.* 2012;9(3):407–13. DOI:10.1016/j.hrthm.2011.09.072.
15. Mizuno A, Miyashita M, Kohno T, Anzai T. Quality indicators of palliative care for acute cardiovascular diseases. *J Cardiol.* 2020;76(2):177–83. DOI:10.1016/j.jjcc.2020.02.010.
16. Barry J. Maron. Clinical Course and Management of Hypertrophic Cardiomyopathy. *N Engl J Med.* 2018;379(20):1977. DOI:10.1056/NEJMc1812159.
17. Kim LK, Swaminathan RV, Looser P, et al. Hospital volume outcomes after septal myectomy and alcohol septal ablation for treatment of obstructive hypertrophic cardiomyopathy: US Nationwide Inpatient Database, 2003-2011. *JAMA Cardiol.* 2016;1(3):324–32. DOI:10.1001/jamacardio.2016.0252.

18. Sigwart U. Non-surgical myocardial reduction for hypertrophic obstructive cardiomyopathy. *Lancet*. 1995 Jul 22;346(8969):211-4. DOI:10.1016/s0140-6736(95)91267-3.
19. Thorsten Lawrenz B, Borchert C, Leuner M, Bartelsmeier. Jens Reinhardt. Endocardial radiofrequency ablation for hypertrophic obstructive cardiomyopathy: acute results and 6 months' follow-up in 19 patients. *J Am Coll Cardiol*. 2011 Feb 1;57(5):572-6. DOI: 10.1016/j.jacc.2010.07.055.
20. G R ter Haar. High intensity focused ultrasound for the treatment of tumors. *Echocardiography*. 2001;18(4):317-22. DOI: 10.1046/j.1540-8175.2001.00317.x.
21. James E, Kennedy. High-intensity focused ultrasound in the treatment of solid tumours. *Nat Rev Cancer*. 2005;5(4):321–7. doi:10.1038/nrc1591.
22. Ruoyu S, Kian TC, Puay HT. Histopathological features of recurrent prostate adenocarcinoma after high intensity focused ultrasound (HIFU) focal treatment: A case report. *Urol Case Rep*. 2021;38:101744. DOI:10.1016/j.eucr.2021.101744.
23. David J, Engel R, Muratore K, Hirata R, Otsuka K, Fujikura K, Sugioka. Myocardial lesion formation using high-intensity focused ultrasound. *J Am Soc Echocardiogr*. 2006;19(7):932–7. DOI:10.1016/j.echo.2006.02.012.
24. Ryo Otsuka K, Fujikura Y, Abe K, Okajima T, Pulerwitz DJ, Engel. Extracardiac Ablation of the Left Ventricular Septum in Beating Canine Hearts Using High-Intensity Focused Ultrasound. *J Am Soc Echocardiogr*. 2007;20(12):1400–6. DOI:10.1016/j.echo.2007.03.007.
25. Schmidt B, Antz M, Ernst S, Ouyang F. Pulmonary vein isolation by high-intensity focused ultrasound: First-in-man study with a steerable balloon catheter. *Heart Rhythm*. 2007;4(5):575–84. DOI:10.1016/j.hrthm.2007.01.017.
26. Elodie Constanciel. WApoutou N'Djin, Francis Bessière, Françoise Chavrier, Daniel Grinberg. Design and evaluation of a transesophageal HIFU probe for ultrasound-guided cardiac ablation: simulation of a HIFU mini-maze procedure and preliminary Ex Vivo trials. *IEEE Trans Ultrason Ferroelectr Freq Control*. 2013 Sep;60(9):1868–83.
27. Ziqi Wu, Madhu SR, Gudur, CX DEng. Transmural ultrasound imaging of thermal lesion and action potential changes in perfused canine cardiac wedge preparations by high intensity focused ultrasound ablation. *PLoS One*. 2013;8(12):e82689. DOI:10.1371/journal.pone.0082689.
28. Yu SC, Cheung EC, Leung VY, Fung LW. Transmural ultrasound imaging of thermal lesion and action potential changes in perfused canine cardiac wedge preparations by high intensity focused ultrasound ablation. *Ultrasound Med Biol*. 2019;45(12):3207–13. DOI:10.1016/j.ultrasmedbio.2019.07.410.c.

Figures



Figure 1

a. the operation control system; b. the treatment bed; c. the treatment probe with a imaging probe; d. the degassed water generate unit

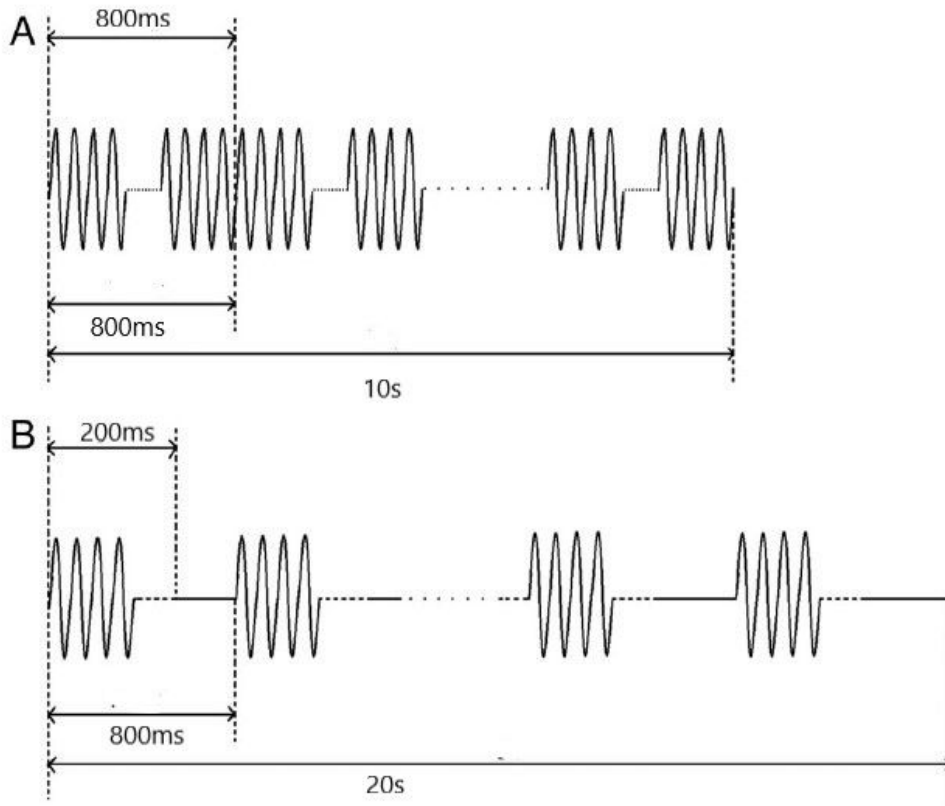


Figure 2

The pulse repetition frequency of each group was 1.03MHz. A: Continuous HIFU (DC, 100%) with a total irradiation time of 10 seconds. B: Pulsed HIFU (DC, 20%) with a power of 400W for 20 seconds with a pulse work of 200ms in 800ms.

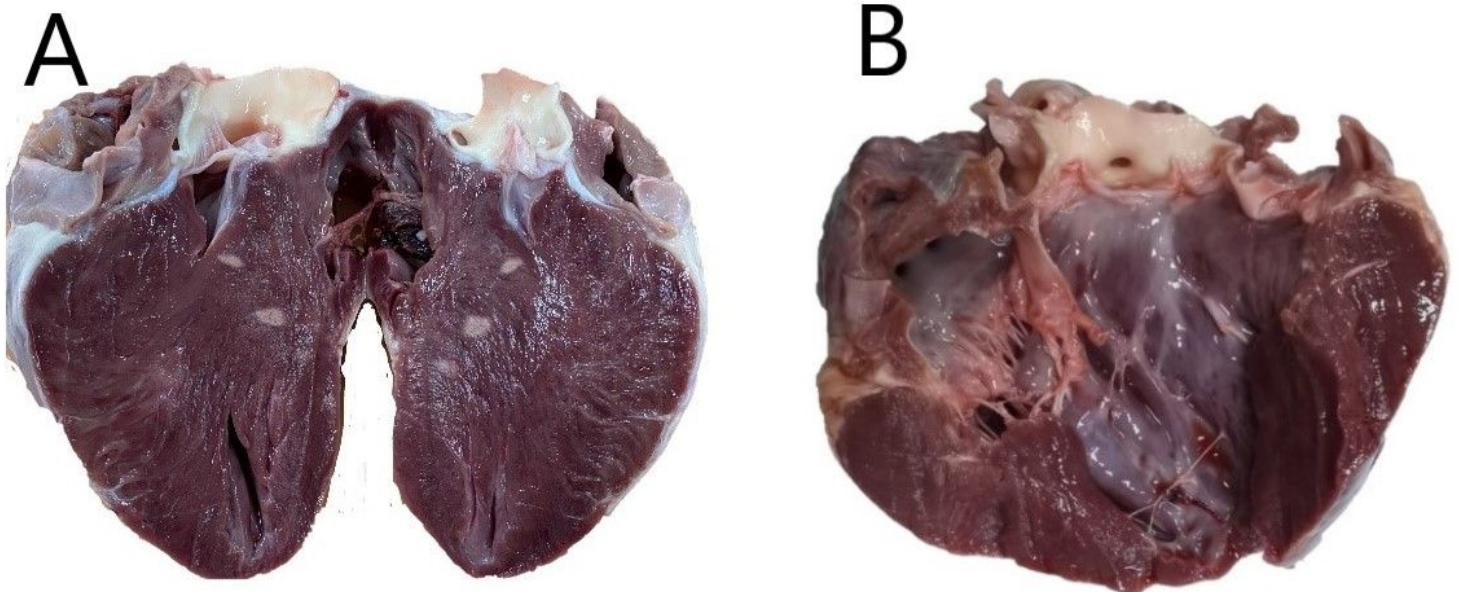


Figure 3

Gross morphologic features of the lesions. A: four coagulative necrotic lesions of different sizes with a clear boundary in the ventricular septum. The color of the necrotic lesion was significantly different from that of the surrounding normal myocardial tissue. B: The endocardial surface was intact, and no significant damage was seen in the endocardial surface.

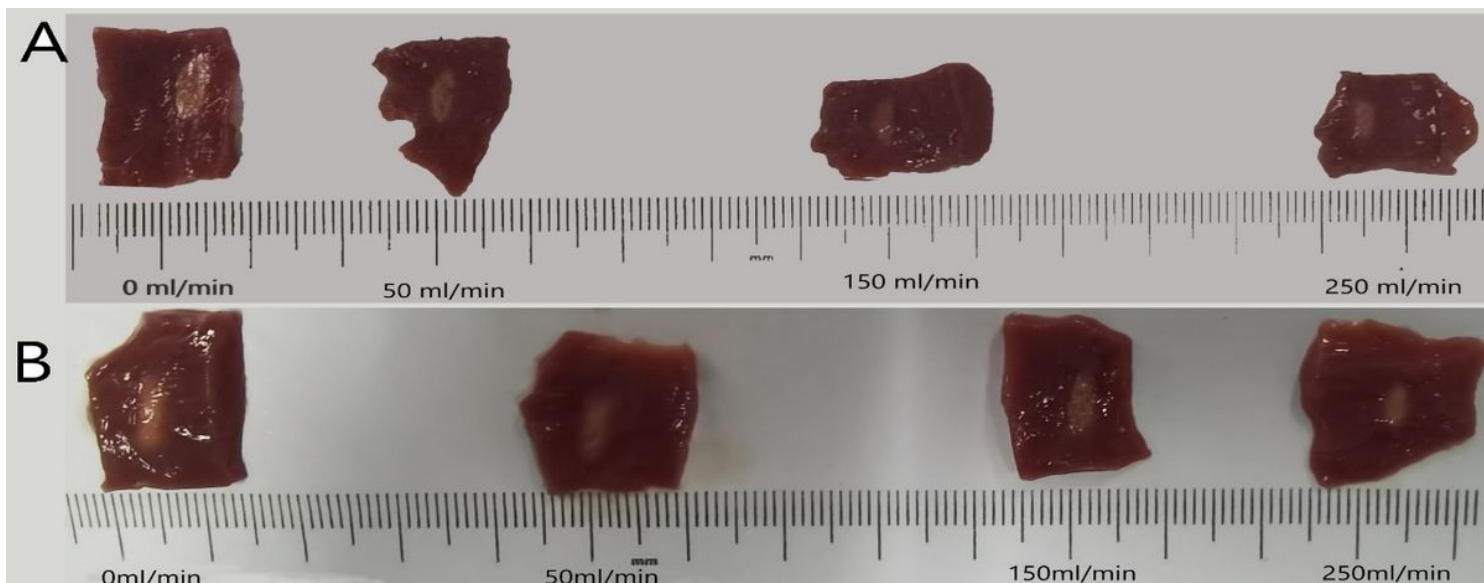


Figure 4

The size of necrotic area under different perfusion flows. A: Tissue after continuous ablation (a power of 200W for 10 seconds); B: Tissue after Pulsed ablation (a power of 400W for 20 seconds with a pulse work of 200ms in 800ms).

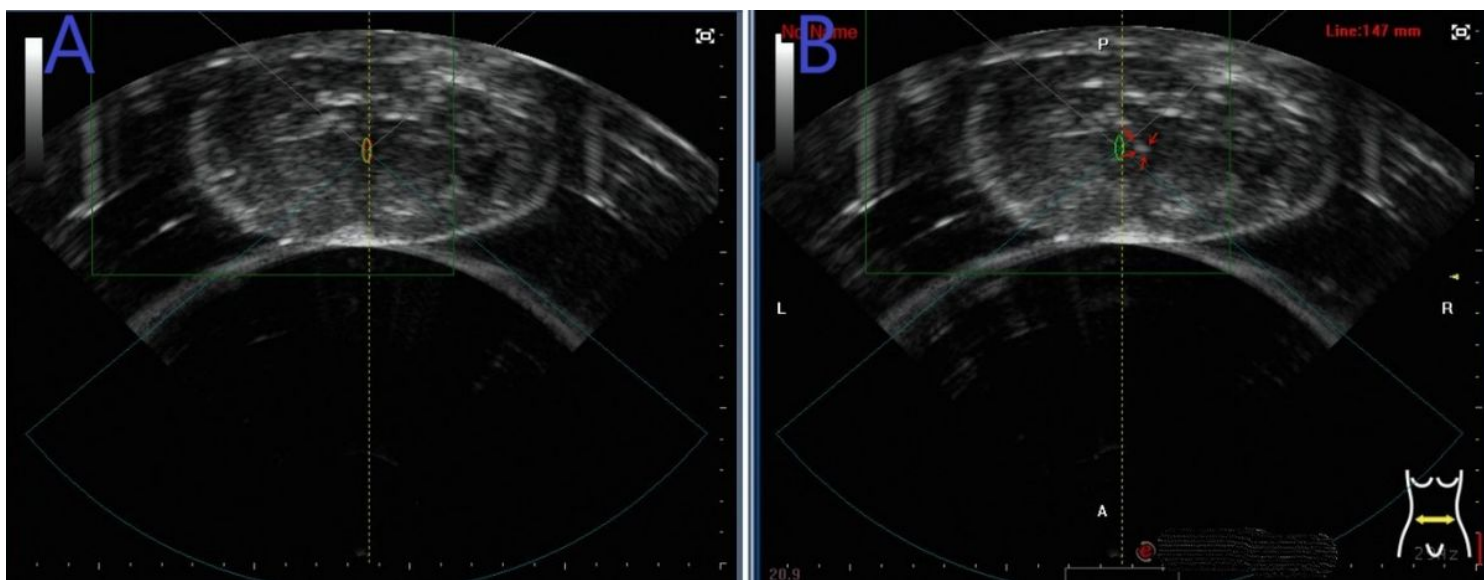


Figure 5

Ultrasonic images of porcine heart during the ablation. A: Guidance of septal ablation using HIFU. The virtual focus of the HIFU (yellow circle) was set at the basal septum by ultrasound guidance. B: Tissue after ablation. Conspicuous gray scale changes (red arrow) could be clearly observed in some samples.

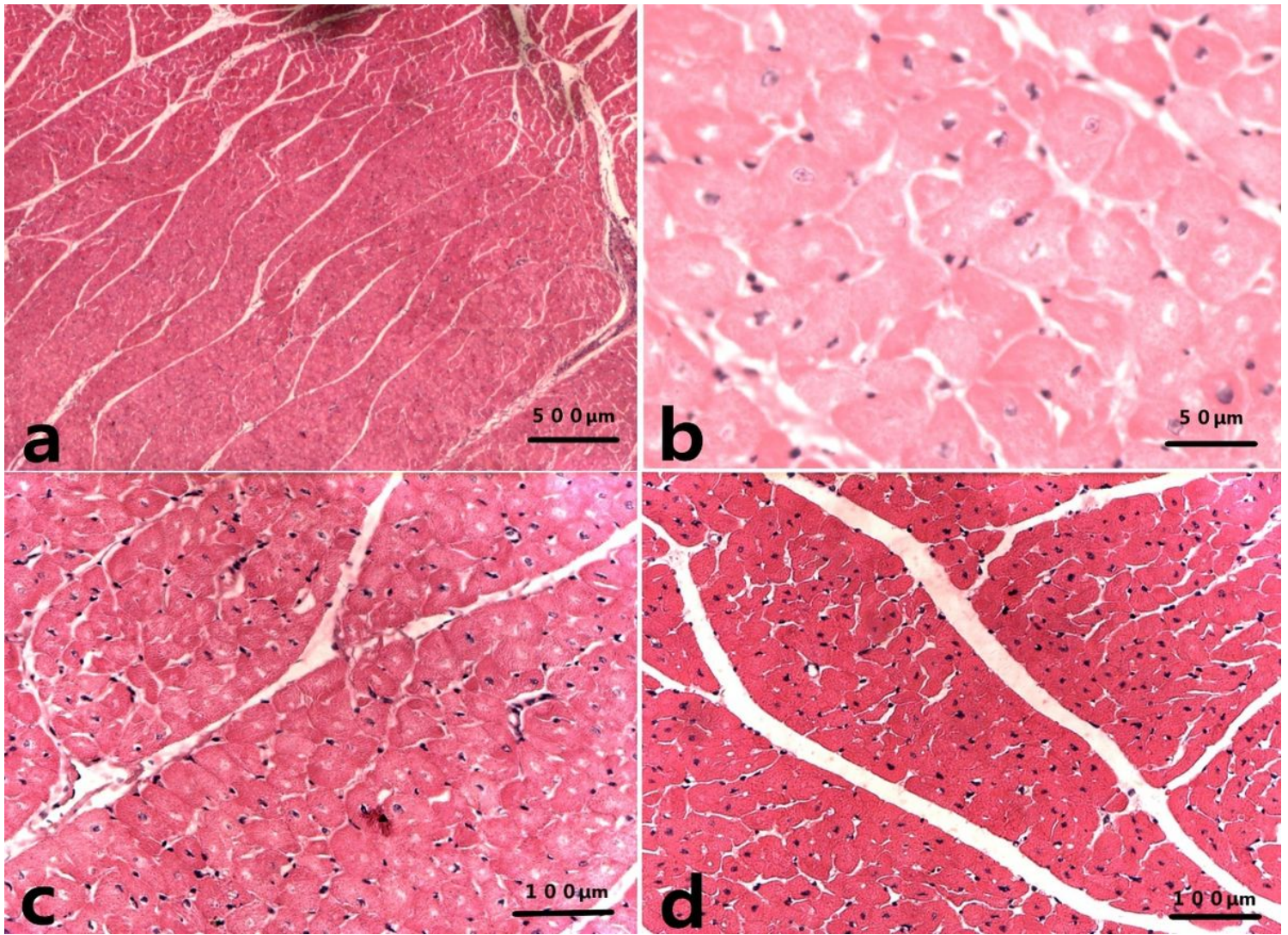


Figure 6

Histologic features of the lesions. a, under low-power microscopy, the lesion was equally lightly stained with a clear boundary. b&c, under high-power microscopy, the cardiomyocyte nuclei disappeared, and the erythrocytes were effused. Karyopyknosis with dark staining was present in the boundary area. d, Peripheral normal myocardial cells were arranged neatly, with complete structure and normal nucleus.